COMBINED ADJUSTMENT OF PHOTOGRAMMETRIC AND GPS DATA

I.Colomina, Barcelona

1 INTRODUCTION

Geodetic positioning techniques will be deeply influenced by satellite geodesy. For certain applications, in certain areas, we are already witnessing the impact of the Global Positioning System (GPS). In some countries in Europe, the high accuracy and density of geodetic networks allow for a smooth transition from classical to satellite based surveying procedures.

In Catalonia the situation is quite different. The first modern –i.e. adjusted– third order network –8-10 Km between adjacent reference points– was not available until 1979 and only in the province of Barcelona. It was only after 1980 that a second order adjusted network –20 Km long average base lines– was made available for the rest of Catalonia [2]. In 1988 the third order densification of the southern areas was finished, so now the situation is as follows: there is a 3rd. order geodetic network available for the 34% of the country (about 380 reference points, or .0272 $points/Km^2$); the remaining 66% is covered with a density of .0045 $points/Km^2$. It is expected that in three years the whole country will be covered with a third order geodetic network (about 900 points).

Nevertheless, from a classical point of view, the estimated number of required reference points to keep up with urban and industrial status and developement ranges between 10000 and 15000 [3]. These points would build up the fourth order geodetic network, for which the *Institut Cartogràfic de Catalunya* (ICC) is responsible.

When the full GPS satellite constellation is deployed a natural question will arise in geodetically developed countries: whether it is still necessary to maintain thousands of geodetic reference points. This general question reads, translated to the particular situation of Catalonia, as whether it is still necessary to set them up.

The answer to this question is still under discussion at the ICC, yet it is becoming more and more apparent that a geodetic network is just a means of geodetic positioning rather than a goal in itself. Then, the alternative approach would be the concept of a GPS-based local positioning system. In addition to the conventional surveying equipement and procedures, the basic constitutive elements of such a system are a geoid model and accurate 3 dimensional relative positioning procedures.

GPS supported aerial triangulation is regarded at the ICC as a particular positioning procedure in the frame of a local positioning system. Other positioning procedures (conventional, static GPS, kinematic GPS, the latter in combination with inertial navigation systems, etc.) are regarded in a similar way. It is the lack of a dense geodetic network together with the intensive use of aerial triangulation for mapping (4500 images per year), which makes this particular technique so interesting for the ICC and the one of the future local positioning system in which more effort is being invested.

2 INTEGRATION OF KINEMATIC GPS DATA INTO PHOTOGRAMMETRIC NETWORKS

The integration of GPS-derived aircraft positions in aerial triangulation aims at replacing ground control by aerial control. Acquisition of aerial control is a highly automated and precise procedure and therefore it is expected to be more cost effective than acquisition of ground control. In other words, one adds to the photogrammetric network a new observable type which leads to a higher network quality or to a reduction of the so far usual number and type of observations. Integration of GPS-derived positions in aerial triangulation seems to be, as well, the most successful attempt to provide direct determination of image exterior orientation elements, in the sense that GPS aircraft positions are closely related to the image projection centers.

42nd Photogrammetric Week, Stuttgart 11-16.9.89.

An ideal operational system would consist of a metric camera together with a GPS receiver which is able to perform phase observations at a high observational rate (1 observation every 0.2-1 s). As the interest is in the coordinates of projection centres at exposure moments, the time at which the images are taken and the time at which the phase is recorded must be related to a common time reference system. And since the camera is maneuvered during flight the relative position of the GPS antenna center with respect to the projection center changes, and must be recorded. After the flight the phase observations are processed and the antenna coordinates are computed for every GPS observation epoch. The coordinates at exposure moments are finally interpolated. Because of the high dynamics of a photogrammetric flight, the determination of the exposure moments and their relation to the phase recording moments is a crucial aspect of the system.

Comprehensive computer simulations [5] were performed under the simplified hypothesis that image projection centers and/or camera attitudes could be observed directly. In spite of this simplification, two main results must be kept in mind. First, the favourable propagation of projection center coordinates precision to the ground point precision. Secondly, attitude data have –for the usual network configurations– only a limited influence. Thus [1][p.27], according to the simulations, the required accuracy of projection centers of a 1 : 4000 photo scale block in order to reach 1-2 cm horizontal accuracy and 6 cm vertical accuracy on ground is just 15 cm assuming a precision of 3 μm in photogrammetric observations.

Other simulation studies dealing with the compensation of systematic errors in GPS-photogrammetric networks and even combining GPS aerial control with DTM ground control are given in [4, 8].

At this point of research, a real block to work with, to check the validity of the theory and to develope suitable computer programs was of the utmost importance.

3 THE RELEVANCE OF THE DUTCH EXPERIMENT: THE FLEVOLAND BLOCK

In june 1987 a photogrammetric testflight consisting of about 360 images at 1 : 3800 scale arranged in 16 parallel strips was performed over an area of 4 $Km \times 4\ Km$ in the Netherlands [10]. The airplane was equiped with a GPS *SERCEL TR5SB* receiver and its corresponding antenna. The camera was a *WILD RC10* which had been modified in order to relate the shutter's maximum aperture moment to the GPS receiver time scale with an accuracy of better than 1 milisecond. The position of the antenna center relative to the projection center was accurately determined and during the flight the camera was held fixed. On the ground, a 3-d network of about 50 points was measured with two GPS *TRIMBLE 4000S* receivers. A second GPS *SERCEL NR52* receiver was placed at one of those ground points to allow for relative kinematic positioning of the airplane. Further information on the flight characteristics and organization can be found in [6,10].

The goals of the experiment were to investigate

- the accuracy of GPS kinematic point determination in high dynamics mode [6] (G1),

and also

- the accuracy of combined GPS-photogrammetric point determination with reduced ground control [10] (G2).

At that moment an accuracy of 10 cm for the antenna centers at exposure moments was expected. In order to check it (G1) a subset of 130 images in 7 strips was chosen (tables 1 and 2) and a particularly *strong* photogrammetric network aimed at a very precise determination of projection centers was designed and observed at the *Institut für Photogrammetrie* (IfP) in Stuttgart. The analysis of this block concerning research aspect G1 is to be found in [6, 7,10]. Some of the results found by Frieß such is the high inner accuracy level of GPS antenna coordinates ($\sigma = 3\ cm$) as well as the existence of systematic drifts which can be linearly modeled, have been starting points for the investigations reported in the following sections. This paper concentrates in research aspect G2.

Again, the relevance of the Flevoland experiment must be emphasized because of the good results concerning G1 and G2 aspects and also because of its usefulness in testing and developing proper mathematical models.

C	*WILD RC10*	n_s	283	C	camera type	n_s	num. of signalised points
		n_n	117			n_s	id. of natural tie points
f	213.67 mm	n_a	477	f	focal lenght	n_a	id. of pugged tie points
h_g	820 m	n_t	877	h_g	flying h.ab.ground	n_t	total number of points
s	1 : 3800			s	photo scale		
v	240 Km/h	n_{go}	3×130	v	airplane speed	n_{go}	number of GPS obs.
p	70 %	n_{DP}	8	p	forward overlap	n_{DP}	id. of drift par. sets
q	50 – 60 %	σ_{SD}	3 – 6 cm	q	side overlap	σ_{SD}	σ of SD solution
		σ_{NA}	4 – 12 cm			σ_{NA}	σ of NA solution
n_i	130			n_i	number of images		
n_{AP}	2	n_{HV}	4	n_{AP}	id. of AP sets	n_{HV}	num. of full control p.
n_s	7	n_V	8	n_s	id. of strips	n_V	id. of vertical c.p.
n_{i_s}	18 – 19	σ	1 – 2 cm	n_{i_s}	id. of photos/strip	σ	σ control points
t	3 s			t	time between exp.		
		$V1$ check-points					
n_{po}	2×5833	n_{HV}	33	n_{po}	num. of photo obs.	n_{HV}	number of full ch.p.
σ_s	2.5 μm	n_H	8	σ_s	σ signalised points	n_H	id. of horizontal ch.p.
σ_n	5 μm			σ_n	σ natural points		
σ_a	7.5 μm	$V2$ check-points		σ_a	σ pugged points		
m_p	6.65	n_{HV}	31	m_p	obs. per point	n_{HV}	number of full ch.p.
m_i	44.87	n_H	8	m_i	obs. per image	n_H	id. of horizontal ch.p.

Table 1: Flevoland block: photogrammetric parameters.

4 THE MATHEMATICAL MODEL

Often, the integration of GPS and from other navigational systems derived data into photogrammetric networks is referred to as the integration of *directly observed camera orientation data*. This is correct since this type of data is so closely related to the camera orientation parameters that for many applications navigational information can be regarded as actual orientation data. From a mathematical point of view this means that the assumed functional model is

$$\mathbf{x}_g^j = \mathbf{X}^j \tag{1}$$

where $\mathbf{x}_g^j = (x_g^j, y_g^j, z_g^j)^T$ are the *observed* coordinates of the position part of the orientation elements and where $\mathbf{X}^j = (X^j, Y^j, Z^j)^T$ are the position unknowns of the orientation parameters. Although in practice a number of other parameters and constants are to be used, this simplified model suffices for any simulation intended at analysing just the influence of navigational information into aerial triangulation. The same holds for attitude data models $\omega_g^j = \Omega^j$, $\phi_g^j = \Phi^j$, $\kappa_g^j = K^j$. Therefore, it must be pointed out that in spite of the following extensions of equation 1 simulation results such those given in [5, 8] remain valid. Only the ground control configuration or the block geometry must be slightly modified as long as there are drifts in the navigational data; a problem that might be solved when the GPS space segment is fully deployed.

If $\mathbf{X}_a^j = (X_a^j, Y_a^j, Z_a^j)^T$ is the excentricity vector of the receiver's antenna center in the j image reference system, $\mathbf{R}^j = (m_{pq}^j)^T$ is the rotation matrix of the j image system, and $\mathbf{X}^j = (X^j, Y^j, Z^j)^T$ is the j image projection center in the ground object (local) reference system, then the coordinates of the receiver antenna in the object system are

$$\mathbf{X}^j + \mathbf{R}^j \mathbf{X}_a^j. \tag{2}$$

If the satellite reference system $-S-$ and the local reference system $-L-$ are related through a general seven parameter transformation,

$$\mathbf{X}_S = \mathbf{X} + (1+\mu)\mathbf{R}\mathbf{X}_L \tag{3}$$

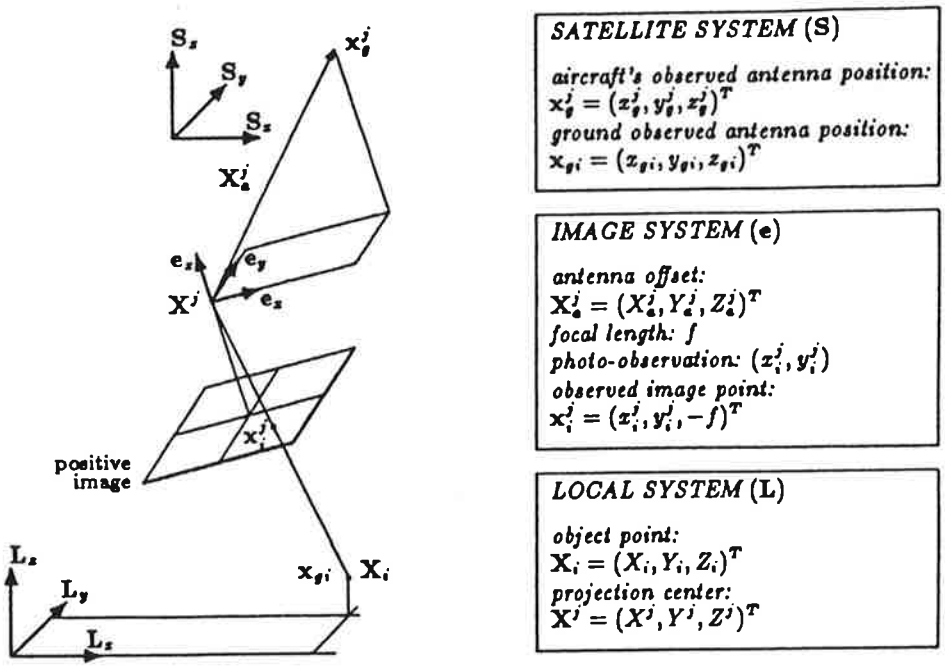

Figure 1: Geometric model for the navigational observation equation.

where $\mathbf{R}$ is the rotation matrix of the L system with respect to the S system, then for the observed coordinates $\mathbf{x}_g^j$ at the j exposure moment the following equation holds

$$\mathbf{x}_g^j = \mathbf{X} + (1+\mu)\mathbf{R}(\mathbf{X}^j + \mathbf{R}^j\mathbf{X}_a^j). \tag{4}$$

Now, if according to the results in [6, 9,10] and also according to the results in table 3, the navigational drifts are linearly modeled the former equation 4 becomes

$$\mathbf{x}_g^j = \mathbf{X} + (1+\mu)\mathbf{R}(\mathbf{X}^j + \mathbf{R}^j\mathbf{X}_a^j) + \mathbf{X}_s + \mathbf{V}_s(t^j - t_s), \tag{5}$$

where $\mathbf{X}_s = (X_s, Y_s, Z_s)^T$, $\mathbf{V}_s = (Vx_s, Vy_s, Vz_s)^T$ are constant and velocity drift parameters for the s parameter set. An image j can only be related to one drift parameter set. t^j is the time at which the j image was taken and it is reduced to a drift set time origin t_s computed as

$$t_s = (\sum_{j=s_1}^{s_k} t^j)/n_s,$$

where the n_s images $s_1, \ldots, s_k$ belong to the drift set s.

If a stationary receiver is used, or if the coordinates of a number of object points in the S system are known, additional observation equations which essentially contribute to the estimation of the datum transfer parameters can be set based on

$$\mathbf{x}_{ig} = \mathbf{X} + (1+\mu)\mathbf{R}\mathbf{X}_i, \tag{6}$$

where $\mathbf{X}_i = (X_i, Y_i, Z_i)^T$ are the coordinates of a ground object point in the L system and $\mathbf{x}_{ig} = (x_{gi}, y_{gi}, z_{gi})^T$ are the observed or known coordinates of the same point in the S system.

Equation 5 represents, in fact, elementary geometrical relationships –see figure 1– but relates 3 observed amounts to 22 unknowns which are highly correlated. This is the situation, for instance, between datum transfer and drift parameters or between the antenna offset $\mathbf{X}_a^j$ and the orientation elements. It seems at least that the antenna offset should be measured input data recorded by any hardware means at each exposure moment, so it can be regarded as a constant in formula 5 or as an observation $\mathbf{x}_a^j$ modelled in the usual way $\mathbf{x}_a^j = \mathbf{X}_a^j$. In the adjustment of the

Flevoland block no one of these problems arose. The GPS data was previously transformed to a local 3-d system so the S system already was the L system. As mentioned, the camera was held fixed during the flight: the offset was accurately measured on the ground and it was introduced in the adjustment through the proper observation equation.

5 THE SOFTWARE

The above functional models for GPS derived coordinate observations together with the conventional selfcalibrating bundle-photogrammetric model have been implemented in a general network adjustment program called ACX (from the catalan *Ajust Combinat de Xarxes* - Combined Network Adjustment).

ACX is intended to be the basic tool for network adjustment in the ICC during the next years. It has been conceived and designed to master any type of geodetic-photogrammetric network, though the first experimental version has been developed and tested only with photogrammetric and GPS-photogrammetric blocks.

Investment in software developement and program performance (i.e. computing time, memory-disk requirements) are crucial aspects when designing such a general tool. In order to keep them within reasonable bounds, special effort has been put into two design points:

1. the definition of a general data structure for geodetic-photogrammetric observations and related data (sensors, auxiliary information,...);
2. the construction of a general mathematical adjustment kernel (formation of design and normal matrices, solution, inversion,...).

Design aspect 1 serves the purpose of software simplicity and reliability. For instance, a unique module prints out residuals of any observation type.

On the other hand, the construction of the adjustment kernel is based on block vector-matrix structures (hyper-vectors and hypermatrices of hypercolumns and hyperrows). Then, general sparse matrix techniques can be used and full advantage of the intrinsic network topology is taken. Organizational questions as the *band-border* structure or the *reduced normal equations*, are just particular ways of sorting the group unknowns. Thus, for the Flevoland block the description data of the normal matrix only requires between 2-6% of the storage required by the factorized matrix itself depending on the parameter sorting.

Realization of design aspect 2 through the above mentioned structures and techniques serves also the purpose of software simplicity. A nice example is that the normal matrix N – about 300000 nonzero elements spread in a sparse symmetric matrix– and $(n-u)\hat{\sigma}_0^2$ –just a single element– are computed by the same module since A^TPA $(=N)$ and v^TPv $(=(n-u)\hat{\sigma}_0^2)$ are similar transposed products between similarly organized matrices.

Because of its flexibility and generality ACX is, as well, a useful tool for the ongoing research. Nevertheless, when the definitive model for the incorporation of GPS aerial control is ready it will be possible to extend most of the old bundle programs.

All results hereafter reported have been obtained with ACX program.

6 BACK TO THE FLEVOLAND BLOCK

In this section the basic network configuration and the different adjustment versions of the Flevoland block which are analysed in section 7 are introduced. As only one control configuration has been investigated, there are

d	ST	SV	ΔT	ΔL	P	σ_{SD}	σ_{NA}
10.6.87	3.1	6 8 9 — 12	26	1.70	40	6	12
	3.2	6 8 9 11 12	32	2.13	3.5	3	4
	4	6 8 9 11 12	58	3.96	3.5	3	4
	5	6 8 9 11 12	63	4.25	3.5	3	4
	6	6 8 9 11 12	62	4.26	3.5	3	4
12.6.87	1	6 8 9 11 12	60	4.02	3.5	3	4
	7	6 8 9 11 12	64	4.25	3.5	3	4
	9	6 8 9 11 12	68	4.45	3.5	3	4

d	date	
ST	photo strip	
SV	observed satellites	
ΔT	photo strip time duration	s
ΔL	photo strip lenght	Km
P	PDOP	
SD	Single Differences solution	cm
NA	Navigation solution	cm
3.1	9 images of strip 3	
3.2	11 images of strip 3	

Receivers: *SERCEL TR5SB & NR52*
Observations: carrier phase
Observation rate: 0.6 s

Table 2: GPS data parameters.

essentially only two different block configurations *SD* and *NA* (section 6.2) intended at answering the question of whether a GPS ground receiver is required or not.

6.1 Ground control configuration

In the area covered by the selected 130 images a 3-d network of 51 reference points was measured with GPS receivers [10][p.416]. They are targeted points and their coordinates were given in the WGS84 reference system and further transformed to a *local horizon* system. In [10], as well, their horizontal error ellipses, whose semimajor axes range between .5 cm and 3 cm, are plotted.

45 points out of the 51 points were selected for block version *V1* after removing 6 points according to the following criteria:

- all points with standard deviations of about 3 cm were disregarded;
- 4 points were flagged as *gross errors* by program *PATB-RS* during the adjustment of a conventional aerial triangulation block where all 51 points were introduced as control points.

Based on these 45 points a minimal ground control configuration was selected. It consists of 4 horizontal and vertical control points schematically located at the block corners and of 2 vertical control chains (4 + 4 vertical control points) located at the block border, at the ends of the strips.

6.2 GPS aerial control configurations *SD* and *NA*

The processing of the Flevoland GPS data is thoroughly described in [6, 7]. Two different block adjustment versions (*SD* and *NA*) corresponding to two different airplane's antenna coordinate sets have bee analysed. In both cases, the broadcast ephemeris were used. In the first solution version (*SD*) the carrier phase observations of both GPS receivers were jointly processed in order to produce relative coordinates of the moving receiver with respect to the stationary receiver. Here, the processing was performed according to the method of single differences. In the second solution version (*NA*) only the observations of the moving receiver were processed.

Finally, the antenna positions at exposure moments were linearly interpolated between the nearest single epoch solutions and the so obtained coordinates were transformed to the local system.

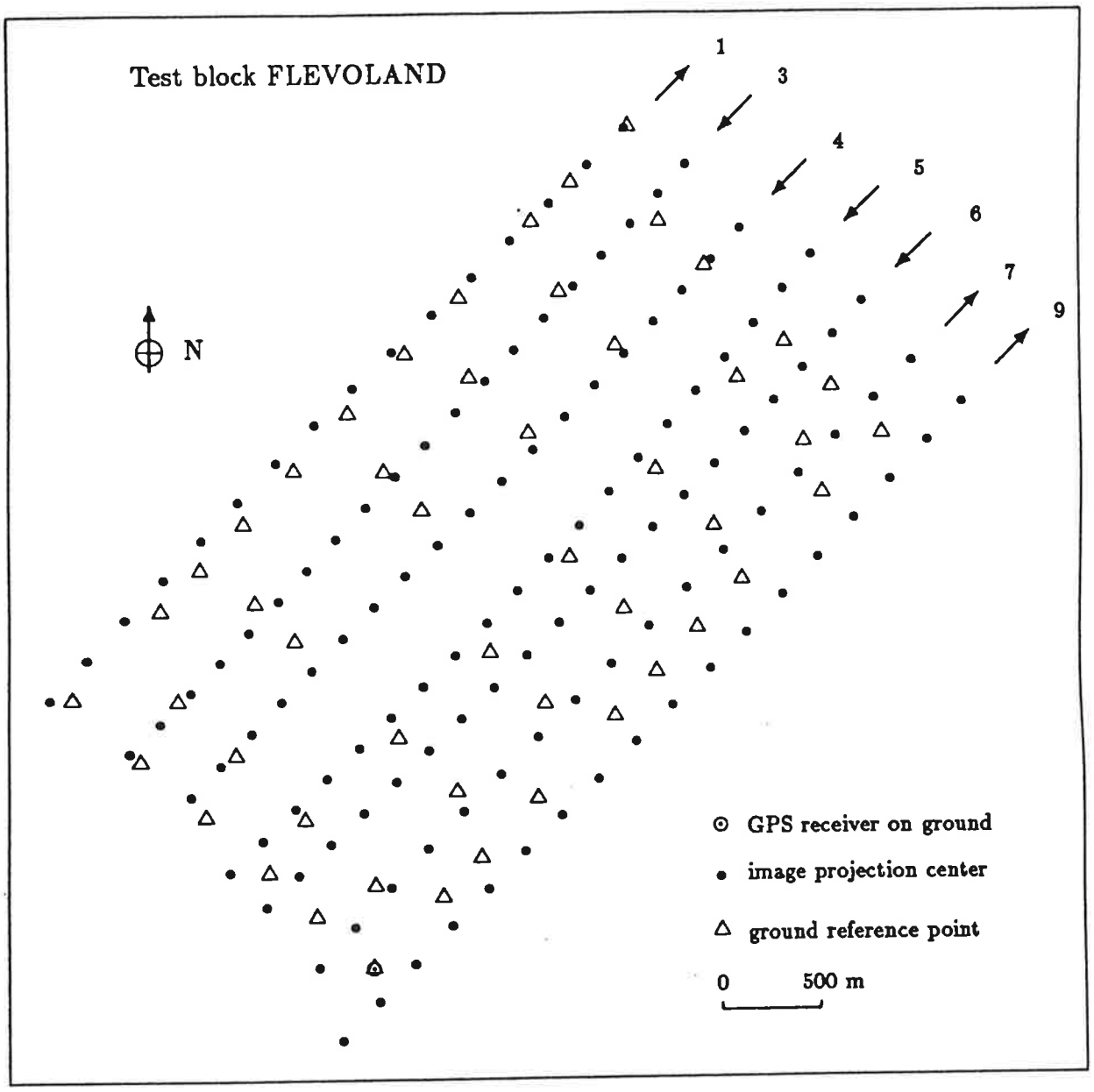

Figure 2: General layout of the block.

6.3 Additional drift parameters

In [7] the empirical accuracy characteristics of the GPS antenna coordinates are studied. One of the conclusions is that a single linear drift parameter set does not suffice to model the drift error if the related GPS data set contains more than one photo strip. The same conclusion was independently made through the results of preliminary combined adjustments just by looking at the adjusted residuals ($\hat{\sigma}_0 \approx 1.4$, where $\hat{\sigma}_0$ is the estimated variance factor since all observations are introduced in the adjustment with a priori realistic weights). Moreover, lock to satellite 11 was lost during photo strip 3 (see table 2) and two different drift sets for substrips 3.1 and 3.2 had to be considered, i.e. a total number of 8 drift parameter sets have been used. Previous adjustments were run in order to select the significant parameters with the Student's t-test (α-level: .05).

6.4 Additional selfcalibration parameters

Two additional selfcalibration sets were utilized –one parameter set per each flight day (see table 2). The Ebner's 12 orthogonal parameters were introduced and checked for significance and determinability before the definitive adjustments were computed. In that respect, a limitation of the block is that the calibrated radial distortions were not available and therefore could not be applied to the observed image coordinates.

6.5 Check-point configurations *V1* and *V2*

All reference points which are not introduced in the adjustment as control are regarded as check-points. Therefore, 41 horizontal check-points and 33 vertical check-points are available. They define block version *V1*.

A second block version *V2* was also defined with only 43 reference points. In this version two more points were removed because of their *suspicious* behaviour in many adjustments and because of their location in the 3-d network. Here, the number of remaining check-points are 39 horizontal and 31 vertical respectively.

6.6 Other *check*-parameters

For the sake of completeness two additional block adjustments were performed using the whole set of reference points as control points. The underlying idea is that for certain parameters which cannot be independently determined –projection centers, drift parameters– the *best* determination is achieved by adjusting the network with as many control points as possible. The reader must be aware of the meaning and limitations of these *check*-parameters. The parameters so computed are orientation and drift parameters, and they will only be used in table 4 in order to analyse how they change when GPS aerial control is introduced and ground control is reduced. *Check* orientation parameters were obtained in a conventional bundle adjustment whereas *check* drift parameters for the *SD* block version were computed in a combined block adjustment. In both cases remaining systematic image errors which cannot be corrected by the used additional selfcalibration parameters do have an influence on the estimated *check* parameters.

7 RESULTS

The empirical accuracy results at check-points are summarized in table 3 and for the adjustment version *SD*, horizontal and vertical residuals are plotted in figure 3. If μ_H, and μ_V are defined as

$$\mu_H^2 = (\sum_{n_H} e_x^2 + e_y^2)/2n_H,$$

and

$$\mu_V^2 = (\sum_{n_V} e_z^2)/n_V,$$

VERSION		SD			NA			SD (no drift par.)		
		x	y	z	x	y	z	x	y	z
V1	m	-0.48	-0.94	0.23	0.44	-0.37	-0.85	8.97	12.80	5.93
	r	2.27	1.92	4.11	2.11	1.84	4.65	9.69	14.45	10.81
	s	2.25	1.70	4.17	2.09	1.83	4.64	3.70	6.79	9.18
	σ	1.06	1.07	1.77	1.08	1.12	1.86	1.48	1.48	2.53
V2	m	-0.31	-0.77	0.94	0.59	-0.23	-0.09	8.93	12.43	6.65
	r	2.16	1.63	3.24	2.10	1.67	3.56	4.69	14.09	10.97
	s	2.17	1.45	3.15	2.04	1.68	3.62	3.79	6.73	8.87
	σ	1.03	1.04	1.73	1.05	1.09	1.82	1.45	1.45	2.51

m: mean value of residuals.

r: root mean value of residuals.

s: empirical std. deviation.

σ : theoretical std. deviation.

Units: *cm*

Table 3: Summary of accuracy results at check-points.

where e_x, e_y and e_z are the differences between adjusted coordinates and given coordinates of n_H horisontal and n_V vertical check points, then for check point configuration *V1* and GPS solution *SD*, the results in table 3 are

$$\mu_H = 2.10\ cm, \quad \mu_V = 4.11\ cm$$

or, in photo scale

$$\mu_H = 5.5\ \mu m, \quad \mu_V = 10.8\ \mu m.$$

Similarly, the corresponding *NA* solution gives

$$\mu_H = 1.98\ cm, \quad \mu_V = 4.65\ cm$$

or, in photo scale

$$\mu_H = 5.2\ \mu m, \quad \mu_V = 12.2\ \mu m.$$

Both *SD* and *NA* results meet accuracy requirements [1][p.27] for large scale mapping and even for numerical point determination, specially $-\mu_H-$ if the contribution of the error of check-points themselves is taken into account. The specialists will also evaluate vertical accuracy without forgetting the focal lenght (213.67 *mm*) and that radial corrections could not be applied. These figures are quite satisfactory for a first practical test and are far beyond initial expectations.

In the third column of table 3 the block empirical accuracy when additional drift parameters are not used is given just to show that they cannot be avoided. A nice thing is that the inadequacy of the functional model without drift modeling could be discovered just by looking at the variance factor $\hat{\sigma}_0$. In that case was $\hat{\sigma}_0 \approx 1.7$ whereas $\hat{\sigma}_0 \approx 1$ when using the proper model.

The no incorporation of drift parameters leads to even worse results than those obtained without auxiliary GPS information and still with the minimal ground control distribution $\mu_H = 2.42\ cm$ and $\mu_V = 11.92\ cm$ (a weak ground control configuration never used for practical applications!).

Another remarkable feature is the high accuracy obtained when the observations made by the receiver on ground were deliberately not used (*NA* solution). This is of especial interest for those who may use this technology in remote or hard accessible areas, or just to reduce expenditures when accuracy requirements are met.

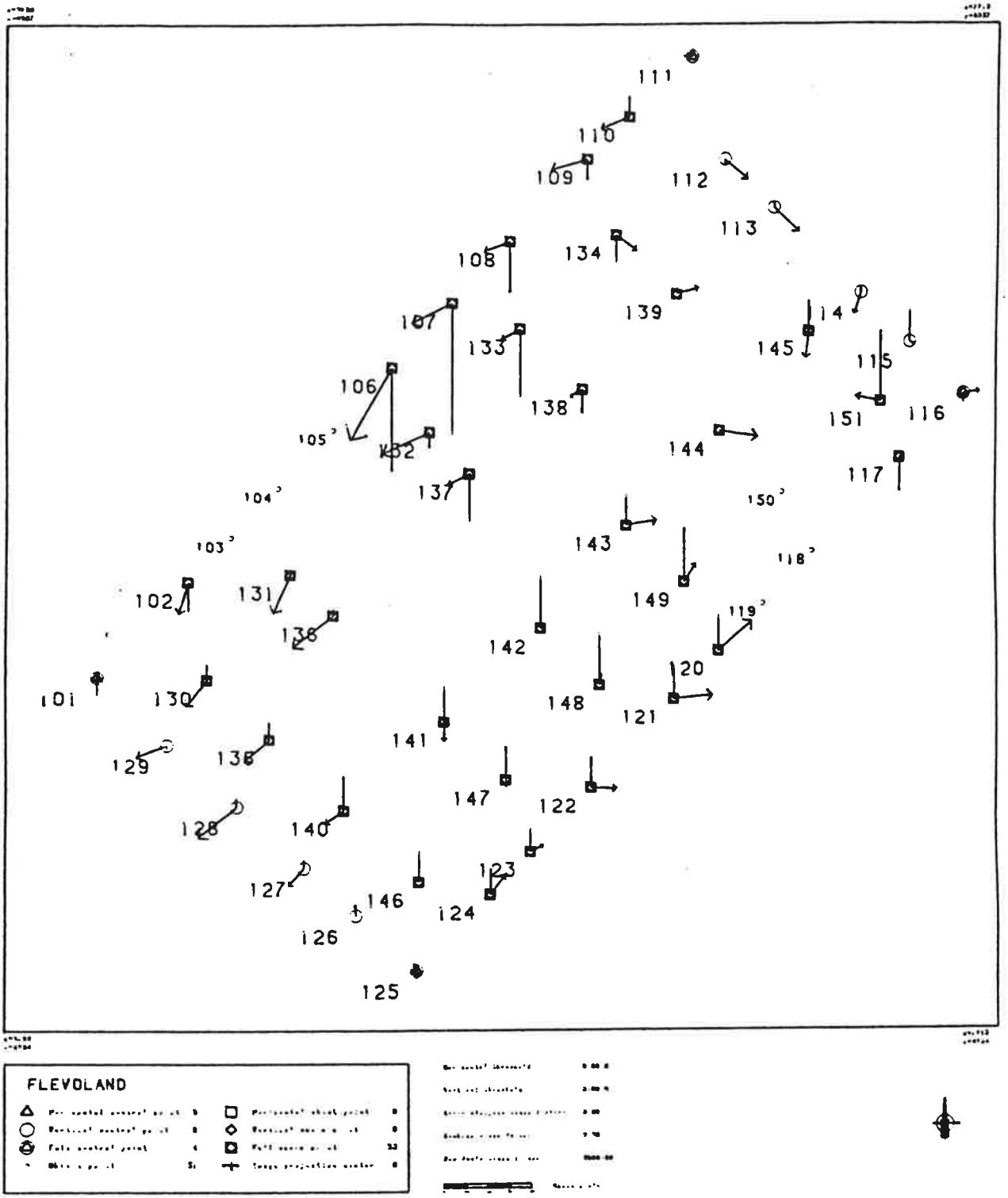

Figure 3: Differences at check-points.

A *surprising* result is that μ_H is larger (*V1* version) for the *SD* solution than for the *NA* solution. Again, the own contribution of check-points' error and the fact that μ_H and μ_V are stochastic amounts with a certain variation range must not be forgotten. *V2* version behaves in a more *reasonable* way.

In table 4 more detailed information is given on version *SD*. Substrip 3.1 exhibits anomalous results (large drifts) as might be already expected. Out of that exception, velocity drifts are typically about 1-3 mm/s. In table 4 .3 the variation of orientation parameters –from conventional aerial triangulation with full ground control to *SD* version– is shown (3 - 5 cm, 1 - 3 $mgon$). It is really small and so is the variation of drift parameters –from combined adjustment with full control to *SD*– (2 cm, 0.5 mm/s).

In figure 3 differences at check points for the *SD* solution are plotted. Local systematic trends can still be seen For the same version, in figures 4 and 5 horizontal and vertical residuals for GPS antenna coordinates can be analysed. They look enough random. Because of the accuracy of check points it is risky to formulate an hypothesis about the remaining –though small– systematic error at check-points but they might originate in still remaining image deformations.

8 CONCLUSIONS

The processing of GPS carrier phase observations has allowed kinematic point determination of aircraft antenna positions which have been succesfully used ($\mu_H \approx 1.9 - 2.1\,cm$, $\mu_V \approx 3.2 - 4.1\,cm$) as aerial control in a combined block adjustment with minimal ground control support. The results indicate that in the near future considerable amounts of effort can be saved by the utilization of this technology which fits well into the requirements found in areas with sparse geodetic networks.

To achieve acceptable results additional drift parameters had to be introduced. Nevertheless, a simple linear model was sufficient, in which case the residuals of the GPS derived antenna coordinates introduced as observations in the adjustment are at the $3 - 4\,cm$ level. Thus, the analysis of the results of the combined adjustment confirms the two main characteristics of the Flevoland GPS data already discussed in [6] and [10]:

- the high inner accuracy of GPS kinematic positioning;
- the existence of systematic drifts which could be linearly modeled in the frame of the block adjustment.

The results justify and encourage further investigations to clarify still open questions which cannot be answered with the Flevoland data:

- the behaviour of the drift error over longer time periods, i.e. over longer photo strips;
- the actual error properties of these hybrid networks on the ground using check-points with a better accuracy to flying height ratio.

Simultaneously, two other questions should be solved on the hardware side: the registration of the relative positions between the camera projection center and the antenna center and the synchronization of the camera to the receiver. Now it is up to the manufacturers not only their realization in the future but also to provide the possibility to upgrade the old equipement.

Last but not least, it must not be forgotten the pure 3 dimensional nature of photogrammetric-GPS networks and if the accuracy potential shown by the results is to be met, suitable at least local geoids should be made available by the responsible institutions.

9 ACKNOWLEDGEMENTS

Many organizations and individuals contributed to the data used for the investigations reported in this article. Without their effort no one of the results of the preceding sections could have been obtained.

The test flight was planned and realised by the Survey Department of Rijkswaterstaat in colaboration with the Technical University of Delft, KLM Aerocarto and SERCEL. Based on this flight a photogrammetric block was designed and observed at the Institute for Photogrammetry (IfP) at the University of Stuttgart. The IfP also processed the GPS carrier phase observations in order to derive the antenna coordinates used in the combined network adjustment. The adjustment software was developed by the author at the ICC and at the IfP in the frame of the Special Research Group *High Precision Navigation* (SFB 228 B5) of the German Research Foundation (DFG).

For the supplied data and for their general cooperation the author wants to express his gratitude.

REFERENCES

/ 1/ Ackermann,F.: The use of camera orientation data in photogrammetry - A review. *Photogrammetria*, Vol. 42, pp. 19-33, 1987.

/ 2/ Caturla,J.L.: La nueva red geodésica de Cataluña, Instituto Geográfico Nacional, Publicación Técnica n' 12, Madrid, 1980.

/ 3/ Colomina,I.: Densificación fotogramétrica de redes geodésicas, VI Asamblea Nacional de Geodesia y Geofísica, Madrid, 1988.

/ 4/ Colomina,I.: High altitude aerial triangulation without ground control. *International Archives of Photogrammetry*, Vol. 27-B9, Comm. III, pp. 215-226, 1988.

/ 5/ Frieß,P.: A simulation study on the improvement of aerial triangulation by navigation data. *International Archives of Photogrammetry*, Vol. 26, Comm. III, pp. 269-283, 1986.

/ 6/ Frieß,P.: Empirical accuracy of positions computed from airborne GPS data. *International Archives of Photogrammetry*, Vol. 27, Comm. III, pp. 215-224, 1988.

/ 7/ Frieß,P.: Arbeiten und Ergebnisse des Teilprojektes B5. *Sonderforschungsbereich 228, Hochgenaue Navigation*, pp. 97-111, 1989.

/ 8/ Grün,A., Runge,A.: The accuracy potential of self-calibrating aerial triangulation without control,1988. *International Archives of Photogrammetry*, Vol. 27, Comm. III, pp. 245-253, 1988.

/ 9/ Seeber,G., Wübbena,G.: Kinematic Positioning with carrier phases and "on the way" ambiguity solution. Presented paper to the Fifth International Geodetic Symposium on Satellite Positioning, Las Cruces, 1989.

/10/ vd Vegt,J.W., Boswinkel,D., Witmer,R.: Utilization of GPS in large scale photogrammetry. *International Archives of Photogrammetry*, Vol. 27-B11, Comm. III, pp. 413-429, 1988.

ABSTRACT

The combined adjustment of conventional photogrammetric observations and new GPS derived coordinate observations closely related to image projection centres makes feasible aerial triangulation with minimum ground control configurations.

The results of a practical GPS-supported aerial triangulation test with a large-scale block are reported. The paper discusses the mathematical model which has been required for the integration of GPS kinematic data into the photogrammetric network and the attained empirical accuracy in ground point determination.

The high accuracy obtained in this experiment ($\mu_H \approx 1.9 - 2.1\,cm$, $\mu_V \approx 3.2 - 4.1\,cm$) indicates that in the future this technique will become routine. The directions of still necessary further research are also given.

KOMBINIERTE AUSGLEICHUNG PHOTOGRAMMETRISCHER UND GPS DATEN

ZUSAMMENFASSUNG

Die kombinierte Ausgleichung konventioneller photogrammetrischer Beobachtungen und neuer GPS abgeleiteten Koordinatenbeobachtungen die eng mit den Projektionszentren verbunden sind, ermöglich uns Aerotriangulation mit einer minimalen Passpunktkonfiguration.

Es werden die Ergebnisse eines praktischen auf GPS gestützten Aerotriangulation mit großem Maßstab beschrieben. Das Papier diskutiert das matematische Modell, das für die Integration der kinematischen GPS Daten in der photogrammetrischen Netz verwendet wurde, und die erzielte empirische Genauigkeit der Punkbestimmung.

Die hohe Genauigkeit, die mit diesem Versuch erzielte wurde ($\mu_H \approx 1.9 - 2.1\,cm$, $\mu_V \approx 3.2 - 4.1\,cm$), zeigt, daß diese Technik in der Zukunft routinemäßig angewandt werden wird. Es wird auch die Richtung vorgegeben, die spätere Forschungsarbeiten einzuschlagen haben.

I.Colomina
Institut Cartogràfic de Catalunya
Balmes, 209-211
E-08006 Barcelona

[1]

Obs. type	x	y	z	Units
Photogrammetric	4.06	5.00	—	μm
Ground control	0.85	0.46	1.12	cm
GPS antenna	2.79	4.39	2.85	cm

[1] Observational residuals

[2] Adjusted drift parameters (cm and mm/s)

[3] Differences at *check* orientation parameters (cm and $mgon$)

[2]

Set number	1	3.1	3.2	4	5	6	7	9	average
X	17.72	-65.58	19.52	—	—	8.66	—	-7.00	
σ_X	2.43	2.68	2.00	—	—	1.37	—	1.85	2.06
Y	57.34	233.25	-24.34	-27.57	-10.27	—	50.09	38.43	
σ_Y	2.64	2.91	2.06	1.62	1.39	—	1.78	2.18	2.08
Z	44.31	-7.81	9.33	7.29	5.49	28.22	38.89	37.50	
σ_Z	3.30	2.89	2.21	2.04	2.08	2.09	2.91	3.07	2.57
Vx	—	—	3.96	1.50	2.12	—	—	-3.12	
σ_{Vx}	—	—	1.44	0.73	0.64	—	—	0.79	0.90
Vy	—	21.89	-3.24	-1.97	—	—	—	2.01	
σ_{Vy}	—	2.88	1.45	0.72	—	—	—	0.72	1.44
Vz	-1.91	—	—	—	—	—	—	—	
σ_{Vz}	0.62	—	—	—	—	—	—	—	0.62

[3]

Parameter	X	Y	Z	Ω	Φ	K
m	-2.42	-1.19	0.01	-0.60	-1.72	0.58
r	5.18	4.31	3.14	3.01	3.41	0.83
s	4.60	4.16	3.16	2.97	2.95	0.59
σ	2.64	2.78	2.61	1.89	1.91	0.81

[4]

Parameter	X	Y	Z
m	-0.48	-0.94	0.23
r	2.27	1.92	4.11
s	2.25	1.70	4.17
σ	1.06	1.07	1.77

[5]

Set number	1	3.1	3.2	4	5	6	7	9
X	4.70	2.29	3.04	—	—	0.41	—	-0.64
Y	0.57	0.35	-0.72	0.44	0.07	—	-0.26	-0.58
Z	2.99	1.30	1.54	0.02	-0.93	-1.45	-2.38	-2.59
Vx	—	—	-0.53	0.56	0.34	—	—	0.43
Vy	—	-1.04	1.00	-0.06	—	—	—	-0.50
Vz	-0.27	—	—	—	—	—	—	—

[4] Differences at check points (cm)

[5] Differences at *check* drift parameters (cm and mm/s)

Table 4: Summary of *SD-V1* block version.

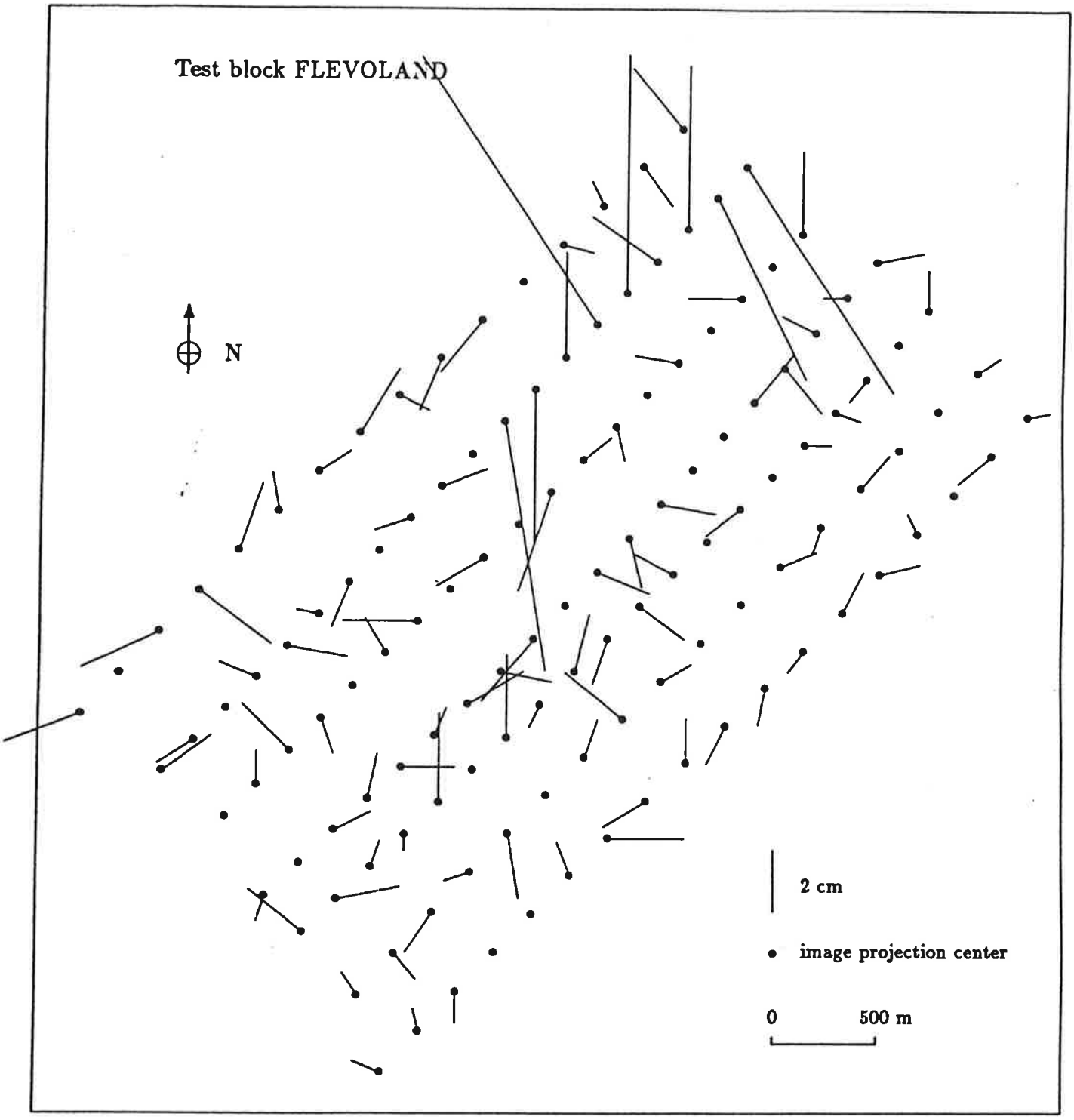

Figure 4: Horizontal residuals of GPS coordinate observations.

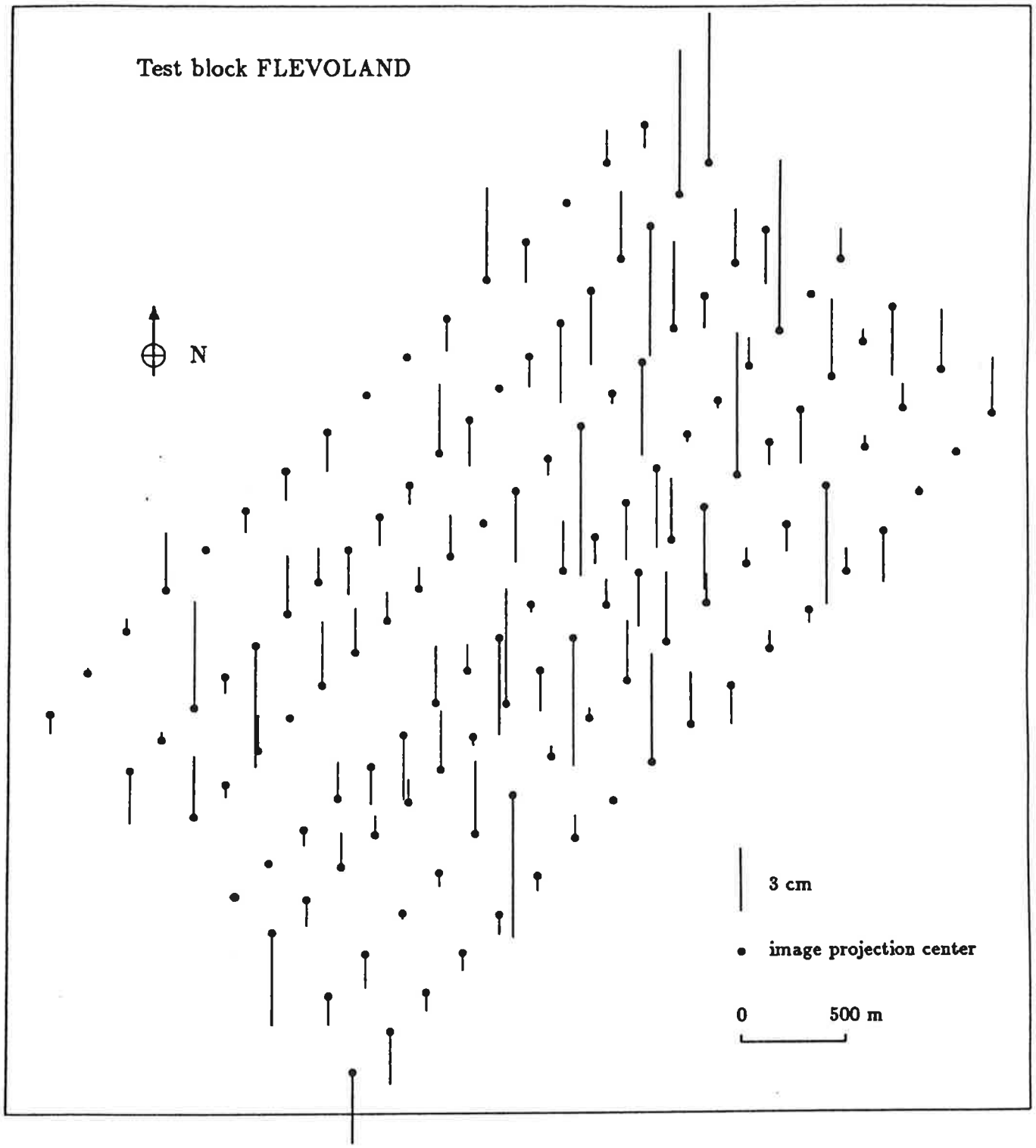

Figure 5: Vertical residuals of GPS coordinate observations.